HHS Public Access

Author manuscript

Dev Neurosci. Author manuscript; available in PMC 2018 October 27.

Published in final edited form as:

Dev Neurosci. 2017 ; 39(6): 507–518. doi:10.1159/000481134.

Sexually dimorphic epigenetic regulation of BDNF in fetal brain in the valproic acid model of ASD

Melissa A Konopko[*,1], **Allison L. Densmore**[*], and **Bruce K. Krueger**[1,+]

Department of Physiology, School of Medicine, University of Maryland Baltimore, 655 West Baltimore Street, Baltimore MD 21201

[1]Program in Neuroscience, University of Maryland Baltimore, 655 West Baltimore Street, Baltimore MD 21201

Abstract

Prenatal exposure to the anti-epileptic, mood-stabilizing drug, valproic acid (VPA), increases the incidence of autism spectrum disorders (**ASD**s); *in utero* administration of VPA to pregnant rodents induces **ASD**-like behaviors such as repetitive, stereotyped activity and decreased socialization. In both cases males are more affected than females. We previously reported that VPA, administered to pregnant mice at gestational day 12.5, rapidly induces a transient, 6-fold increase in BDNF protein and mRNA in the fetal brain. Here we investigate sex differences in the induction of *Bdnf* expression by VPA as well as the underlying epigenetic mechanisms. We found no sex differences in the VPA stimulation of total brain *Bdnf* mRNA as indicated by probing for the BDNF protein coding sequence (exon 9); however, stimulation of individual transcripts containing two of the nine 5'-untranslated exons (5'UTEs) in *Bdnf* (exons 1 and 4) by VPA was greater in female fetal brains. These *Bdnf* transcripts have been associated with different cell types or subcellular compartments within neurons. Since VPA is a histone deacetylase inhibitor, covalent histone modifications at *Bdnf* 5'UTEs in the fetal brain were analyzed by chromatin immunoprecipitation. VPA increased acetylation of multiple H3 and H4 lysine residues in the vicinity of exons 1, 2, 4, and 6; minimal differences between the sexes were observed. H3 lysine 4 trimethylation (H3K4me3) at those exons was also stimulated by VPA, moreover, the VPA-induced increase in H3K4me3 at exons 1, 4, and 6 was significantly greater in females than in males; i.e., sexually dimorphic stimulation of H3K4me3 by VPA correlated with *Bdnf* transcripts containing exons 1 and 4, but not 6. Neither H3K27me3 nor cytosine methylation at any of the 117 CpGs in the vicinity of the transcription start sites of exons 1, 4 and 6 was affected by VPA. Thus, of the six epigenetic marks analyzed, only H3K4me3 can account for the sexually dimorphic expression of *Bdnf* transcripts induced by VPA in fetal brain. Preferential expression of exon 1- and exon 4-*Bdnf* transcripts in females may contribute to sex differences in **ASD**s by protecting females from adverse effects of genetic variants or environmental factors such as VPA on the developing brain.

[+]Corresponding author: Bruce K. Krueger, PhD., Department of Physiology, University of Maryland School of Medicine, 655 West Baltimore Street, Baltimore, MD 21201, bkrueger@som.umaryland.edu, Phone: 410 70 5065, Fax: 410 706 8341.

[*]These authors contributed equally to this research

CONFLICT OF INTEREST STATEMENT

The authors report no conflicts of interest.

Keywords

Autism; autism spectrum disorder (ASD); brain-derived neurotrophic factor (BDNF); DNA CpG methylation; female protective effect; gene transcription; histone modifications; sex-linked; RNA splicing; VPA

INTRODUCTION

Autism spectrum disorders (ASDs) are neurodevelopmental disorders of cognition and behavior that are four-times more prevalent in males than females. The cause of ASDs is unknown, as is the molecular basis for the male sex bias. Although diagnosis usually does not occur until the second year, recent evidence suggests that the disorder is caused by errors in fetal brain development occurring early in pregnancy [1–3]. Recent research has revealed a wide variety of genetic variants that are associated with ASDs and a few single-gene mutations with ASD co-morbidities [4,5]. In addition, *in utero* exposure to environmental factors such as pollutants, toxins, maternal infection and some drugs also increases the probability of an ASD diagnosis, particularly when the pregnant woman is exposed during the first trimester [6–8]. One such environmental factor is valproic acid (VPA), a commonly prescribed anti-epileptic and mood-stabilizing drug [9], *in utero* exposure to which increases the risk of ASDs from 0.5 – 1% in unexposed children up to about 10% [10–15]. The link between VPA exposure and ASDs has led to a widely-used rodent model: a single injection of VPA into pregnant mice or rats (typically at E12 – E13) leads to ASD-like behaviors in the offspring [16–18], including decreased social interactions and repetitive stereotyped behaviors. VPA also induced reductions in cortical thickness and dendritic branching and other anatomical defects similar to those seen in human ASDs [16,19–22]. Additionally, the rodent VPA model mimics the male sex bias in ASDs [23–25].

We previously found that administration of VPA at E12.5 induces a transient, 6-fold increase in *Bdnf* mRNA and BDNF protein expression in the fetal mouse brain [26]. The developing brain is highly sensitive to changes in this key neurotrophin due to its roles in regulating neurogenesis, neuronal differentiation and synapse formation [27]. Whether increased BDNF expression at this developmental stage is pathogenic or protective is not known. *Bdnf* transcription can be initiated from 9 different promoter regions [28], each controlling its own 5'-untranslated exon (5'UTE), which is spliced to a common protein coding sequence (exon 9; Ex9) during transcription, allowing detection of the exon-specific transcripts by PCR [28] (*c.f.*, Fig. 1, inset). We also found that, of the nine 5'UTEs in mouse *Bdnf*, only three (Ex1, Ex4, and Ex6) were detected in fetal brain and expression of all three was stimulated by VPA, suggesting that VPA promotes BDNF expression by activating transcription of those promoters. In those studies, we did not distinguish between males and females; consequently, in the present study, male and female brains were analyzed separately.

VPA has several potential mechanisms of action, one of which is to inhibit class-1 histone deacetylases (HDACs) [29,30]. This activity would be predicted to increase histone acetylation [31], generally a transcription-activating epigenetic mark [32,33]. Several lines of evidence have led to the conclusion that it is the HDAC-inhibiting properties of VPA that induce the ASD-like phenotype after *in utero* exposure [20,34,35]; e.g., prenatal exposure to

structurally-unrelated class-1 HDAC inhibitors, such as trichostatin A (TSA), leads to ASD-like behavior [35]. TSA has also been reported to increase *Bdnf* expression in a neuronal cell line [36].

The evidence that HDAC inhibition *in utero* can induce *Bdnf* expression in the fetal brain and ASD-like behavior in postnatal animals led us to examine epigenetic changes in *Bdnf* Ex1, Ex4 and Ex6 and their respective upstream promoter regions, Pr1, Pr4 and Pr6, in the fetal brain after *in utero* exposure to VPA. Epigenetic changes in Ex2, which is expressed at extremely low levels in the E12.5 brain [26], were also investigated. The effect of VPA on H3K9/14, H3K27 and H4K5/8/12/16 acetylation at these sites was analyzed by native chromatin immunoprecipitation (ChIP). Because there can be "cross-talk" among epigenetic modifications [37,38], we also studied H3K27 and H3K4 trimethylation, which are generally silencing and activating marks respectively. Previous studies showed that there are abnormal patterns of global DNA methylation in ASD brains [39] and the *Bdnf* gene can be regulated by this epigenetic mark [40,41]; consequently, we also analyzed DNA CpG methylation up- and downstream from the Ex1, Ex4 and Ex6 transcription start sites (TSSs). To identify mechanisms that might underlie the increased prevalence of ASDs in males [42], we analyzed VPA-induced *Bdnf* mRNA expression and epigenetic changes in *Bdnf* in fetal brains from both sexes independently.

In this report, we identify molecular consequences of *in utero* VPA exposure on the fetal brain, using an animal model that recapitulates many behavioral characteristics as well as the sex bias of human ASDs. The long-term goal of the study is to generate hypotheses for the cellular and molecular origins of ASDs that can be further tested in other mouse strains, more advanced species and, eventually, in humans.

MATERIALS AND METHODS

Animal Breeding and Tissue Collection

All experiments were conducted according to a protocol approved by the IACUC at the University of Maryland School of Medicine. Timed pregnant C57Bl6 mice were supplied by the University of Maryland School of Medicine Veterinary Resources division; breeding stock was obtained from Jackson Laboratories, Bar Harbor, ME. Pregnancies were timed by overnight breeding. Males and females were separated the following morning (E0.5). At E12.5, pregnant dams were injected intraperitoneally with 400 mg/kg VPA (#P4543, Sigma, St. Louis MO) in sterile-filtered phosphate buffered saline (PBS; 138 mM NaCl/2.7 mM KCl/10 mM Na-phosphate, pH 7.4) or PBS alone and euthanized by cervical dislocation after 3 hrs or 24 hrs. Fetuses were determined to be at Theiler stage 20–21 with an average crown-rump distance of 9.8 mm, consistent with E12.5 [43]. Whole fetal brains, from the telencephalon through the metencephalon, were collected in ice cold PBS together with an additional tissue sample for sex determination of each fetus. 5 mM sodium butyrate was added to the PBS when the tissue was to be used for ChIP. Tissue was frozen on dry ice and stored at −80°C until use. Samples for RNA analysis were homogenized in Qiazol (Qiagen, Valencia, CA) and then frozen. 67 female and 67 male E12.5 fetuses were analyzed for this study.

Fetal Sex Determination

DNA was extracted from a somatic tissue sample using the Quick gDNA Mini- Prep kit (#D3025, Zymo Research, Irvine, CA) and analyzed by PCR using primers for *Gapdh* and *Sry* (Supplementary Table 1A). Adult male mouse DNA was used as a positive control (Supplementary Fig. 1).

Bdnf mRNA Expression

RNA was extracted from brain samples collected 3 hours after *in utero* exposure to VPA using the RNeasy Mini Kit (#74104, Qiagen), including the on-column DNase step. The mRNA was then reverse-transcribed using the High-Capacity cDNA Reverse Transcription Kit (# 4368814, Applied Biosystems, Carlsbad CA) with RNase Inhibitor (#N8080119, Applied Biosystems). The expression level of each 5'UTE was analyzed by qRT-PCR (ViiA 7, Applied Biosystems) using primers listed in Supplementary Table 1B. The forward primer was located in the 5' exon and the reverse primer in the *Bdnf* coding region in order to selectively amplify the spliced RNA (*c.f.*, Fig. 1 inset). The standard curve of serial dilutions for each target had a slope of 1.9 – 2.0 and all data points fell on the standard curve. All data were normalized to β-actin.

Native Chromatin Immunoprecipitation (ChIP)

The protocol used in this study was modified from the Epigenome Network of Excellence (NoE) protocol [44] for reduced tissue sample size. For each ChIP reaction, two sex-matched fetal brains from different litters were pooled. This pooled sample was lysed and nuclei were isolated on a sucrose gradient. Nuclear DNA was sheared by micrococcal nuclease (MNase #M0247S, New England Biolabs, Ipswich, MA). Following centrifugation, the supernatant (*S1*) was collected and the pellet was resuspended and dialyzed overnight in a Tube-O-Dialyzer (G-Biosciences, St. Louis, MO). The dialyzed sample (*S2*) was combined with *S1* and used for both immunoprecipitation and to verify shearing efficiency by agarose gel electrophoresis (see below). 5 μg was of sample were added to DNA-LoBind tubes (#022431021, Eppendorf, Hauppauge, NY) for each antibody; IgG was used as a negative control. Samples were incubated overnight with magnetic protein A coated beads (Millipore, cat # 16-661) and antibodies against H3K9/14ac (#17-615, Millipore, Temecula CA /#C154100200 Diagenode, Denville NJ), H3K27ac (Diagenode #C15410196), H3K27me3 (Diagenode #C15410195), H3K4me3 (Diagenode #15410003) and H4K5/8/12/16ac (Millipore #06-866) or control IgG (#02612, Invitrogen, Waltham MA). The beads were then subjected to three salt washes followed a salt-free wash, which was conducted in a new tube. Chromatin was eluted using an SDS-containing buffer with proteinase K at 55° for 1 hour. DNA was purified from the eluted sample using the MinElute PCR Purification Kit (#28004, Qiagen). Covalent histone modifications were quantified by qRT-PCR; primers (Supplementary Table 1C) were located within the promoters or 5'UTEs of the *Bdnf* gene (Fig. 1, inset). Less than 0.05% of the starting amount of target DNA was detected by ChIP using IgG.

Agarose Gel Electrophoresis

To verify the efficiency of MNase digestion, the combined *S1* and *S2* sample was run on an agarose gel. 0.1% SDS was added to 2 μg of sample and gels were run at 100V for 1.5 hours and post-stained in 1 μg/ml ethidium bromide. The size of the majority of chromatin fragments was between 100 to 300 bp (Supplementary Fig. 2).

Bisulfite Sequencing

DNA was extracted from individual fetal brains using the Quick gDNA Mini-Prep kit (#D3024, Zymo Research). The DNA underwent bisulfite conversion using the EZ DNA Methylation Lightning kit (#D5020, Zymo Research). DNA was PCR amplified using primers constructed with an M13 tag attached to primers to the converted sequence (Supplementary Table 1D). Converted primers were designed using Meth- Primer. DNA was sequenced using the M13 tag to maximize read length.

Data Analysis and Statistics

ChIP data from male and female fetal brains were analyzed by two-way ANOVA with post-hoc Tukey test. Transcript data from qRT-PCR, separated by sex, was analyzed by two-way ANOVA. For DNA CpG methylation analysis, chromatograms (*c.f.*, Fig 5B) were analyzed using Mutation Surveyor (SoftGenetics, State College, PA). For bisulfite-treated DNA, the program compares relative levels of methylated cytosines, read as cytosines, versus unmethylated cytosines, read as thymines. The software determined the “noise” level for each chromatogram and only recognized locations where the methylation level was above that level. Therefore, CpGs with very low levels of methylation would not be identified by this method. The level of methylation at each detected location was analyzed by t-test. Statistical tests were performed on SigmaPlot (Systat Software, San Jose CA). Statistically significant differences are indicated by asterisks as defined in the figure legends. In Figs. 1, 5 and 6, “n” refers to individual fetuses; in Figs. 2 – 4, “n” refers to pooled samples, each containing two fetal brains of the same sex from different pregnancies. A full statistical analysis is provided in Supplementary Tables 2 – 4.

RESULTS

Sex differences among Bdnf transcripts

The effect of VPA on *Bdnf* Ex9 expression is shown in Fig. 1A. Ex9 encodes the BDNF protein and its expression reflects the total level of *Bdnf* mRNA, regardless of the 5’UTE from which transcription is initiated (see Fig. 1, inset). VPA exposure induced an increase in *Bdnf* mRNA in both male and female fetal brains, consistent with the 6-fold increase in Ex9 mRNA previously reported without taking sex into account [26]. We also analyzed expression of Ex1-, Ex4- and Ex6-containing transcripts in both male and female fetal brains (Fig. 1B–D). The effect of VPA on *Bdnf* transcripts containing Ex1 and Ex4, but not Ex6, was sexually dimorphic: a larger stimulation by VPA was observed in female than in male fetuses. Although the qRT-PCR reactions were not calibrated by doping with RNA standards, we estimate that Ex6 was the most abundant *Bdnf* transcript based on C_T values. Since levels of Ex6 were the same in males and females (Fig. 1D), this may explain the

absence of a significant sex difference in Ex9 (Fig. 1A). Consistent with previous findings [26], Ex2-containing transcripts were expressed at levels too low to be quantified using these methods (data not shown).

Histone acetylation

Chromatin from fetal brains was subjected to native ChIP using antibodies to H3K9/14ac, H3K27ac and H4K5/8/12/16ac or control IgG. The immunoprecipitated DNA was analyzed by qRT-PCR to amplify sequences upstream from the TSSs of Ex1, Ex4, and Ex6 (i.e., in the promoter region: Pr1, Pr4, and Pr6) as well as sequences in the 5'UTEs, up to 300 bp downstream from the TSSs (Ex1, Ex2, Ex4 and Ex6) (Supplementary Fig. 3).

Data for histone acetylation are shown in Fig. 2 with male and female fetal brains analyzed separately. At 3 hrs, VPA increased the level of acetylation of H3 at K9/14 and K27 and H4 at one or more of the 4 known acetylated lysines (K5/8/12/16). All data were normalized to the starting amount of target DNA (% Input) for each ChIP. The average stimulation of histone acetylation by VPA across all targets in *Bdnf* was 4.5 ± 1.5-fold. Acetylation of histone lysines analyzed in E2 is also substantially increased by VPA. With the exception of small effects of sex in H3K9/14ac at Ex4 and Ex6 and H3K27ac at Ex6, no sex differences were observed.

We also examined H3K27ac and H4K5/8/12/16ac levels 24 hrs after VPA exposure, by which time the VPA-induced acetylation had returned to control levels; no sex differences were observed (Fig. 3). This parallels the reversal of the VPA-induced increases in *Bdnf* Ex9 mRNA and BDNF protein levels by 24 hrs [26].

Histone methylation

VPA significantly increased H3K4me3 within 3 hrs at each of the seven *Bdnf* sites studied (Fig. 4A). However, in contrast to H3 and H4 acetylation, analysis of H3K4me3 revealed a striking sexual dimorphism. H3K4me3 was significantly higher in females at 5 of the 7 sites examined; notably, in males, VPA had no effect at all on H3K4me3 at Pr4, Pr6 and Ex6. In contrast to H3K4me3, H3K27me3 was unaffected by VPA exposure at any of the sites examined; no sex differences were observed (Fig. 4B).

DNA CpG Methylation

DNA extracted from fetal brains was obtained 3 hrs after administration of VPA to the pregnant dam was bisulfite-modified. Overlapping sequences of bisulfite-converted genomic DNA covering CpGs in the vicinity of the TSSs of Ex1, Ex4 and Ex6 (Fig. 5A) were amplified by PCR using primers specific for bisulfite-converted DNA (Supplementary Table 1D). PCR products were sequenced and the extent to which each unmethylated CpG cytosine was converted to uracil (read as thymine after PCR amplification) was quantified. After bisulfite conversion, methylated Cs continue to be read as Cs. A typical sequencing chromatogram illustrating both unmethylated and partially methylated Cs in Pr4 are shown in Fig. 5B. Of the 117 CpGs in the promoters and coding regions of Ex1, Ex4 and Ex6, 113 were <10% methylated and VPA did not affect the degree of methylation; the locations of these CpGs in *Bdnf* are shown as black ticks in Fig. 5C.

In contrast, a sequence of four CpGs in Pr4 upstream of the Ex4 TSS was 30 – 50% methylated in control brains (red ticks in Fig. 5C). Fig. 6A shows the DNA sequence surrounding this 4-CpG cluster (arrows) which is located just upstream from the Ca^{2+}-regulatory elements in Pr4. These elements are designated CaRE1 – 3 [45] and include the CREB-binding element, *cre* (CaRE3), shown in pink highlighting (Fig. 6A). The effect of VPA on the four hyper-methylated CpGs in Pr4 is shown in Fig. 6B. VPA did not significantly affect methylation of any of the individual CpGs although it significantly reduced the aggregate level of methylation of the cluster; there was no difference between males and females (data not shown).

DISCUSSION

Rationale for analyzing multiple epigenetic marks in *Bdnf*

Although VPA is an HDAC inhibitor, DNA CpG methylation and histone methylation as well as histone acetylation were examined because multiple epigenetic marks act cooperatively in gene activation and silencing, in part due to functional “cross-talk” among these epigenetic mechanisms [32,37,46,47]. For example, acetylated histone lysines can recruit histone methylating or demethylating enzymes to the chromatin, where they would modulate histone methylation levels; more-over, the histone methylase, MLL4, is associated with multiprotein complexes that bind to acetylated histone 3 [48]. An additional factor is mutual exclusion of modifications at the same histone lysine residue, for example, acetylation and trimethylation of H3K27 are mutually exclusive [49]. In addition to crosstalk between histone modifications, histone acetylation can affect DNA CpG methylation by recruiting enzymes that control DNA methylation state [50–52]. Consequently, we examined histone acetylation and methylation, as well as DNA CpG methylation in the vicinity of the TSSs of *Bdnf* 5’UTE’s 1, 2, 4 and 6.

Sexually dimorphic trimethylation of H3K4 induced by VPA

We analyzed the effect of VPA on H3K4me3, an activating epigenetic mark, and H3K27me3, a silencing mark, in both male and female fetuses. We found that stimulation of H3K4me3 by VPA was greater in females than in males at 5 of the 7 sites examined (Fig. 4A). In fact, at Pr4, Pr6 and Ex6, VPA stimulated H3K4me3 in females but had no effect in males. The most dramatic sex differences in the effects of VPA on H3K4me3 were observed at Ex6 (Fig. 4A), despite the fact that no sex differences were observed in Ex6–Ex9 transcripts (Fig. 1). Consistent with this observation, in a study of the chromatin states of male and female adult mouse liver, sex differences were found in activating or repressing histone marks that were not reflected in the corresponding transcripts [53]. Similarly, while widespread sex differences have been found in H3K4me3 levels in a sexually dimorphic region of the adult mouse brain (bed nucleus of the stria terminalis and preoptic area); only 10 – 15% of those genes displayed sexually dimorphic mRNA expression [54]. Therefore, the lack of correlation between sex differences in H3K4me3 and transcript expression as we observed for Ex6, appears to be the norm, while the correlated sexually dimorphic H3K4me3 and transcript expression we observed for exons 1 and 4 are exceptions.

While each of the sites examined in *Bdnf* was found to be associated with substantial levels of H3K27me3, VPA did not alter these levels nor were any sex differences observed (Fig. 4B). Thus, it appears that transcription of these *Bdnf* 5'UTEs is regulated by "poised" promoters [49,55], with increased H3K4me3, but not decreased H3K27me3, contributing to the mechanism by which they can be activated by VPA.

VPA induces robust and widespread histone lysine acetylation at *Bdnf* exons 1, 2, 4 and 6

A working hypothesis for this study was that the stimulatory effects of VPA on *Bdnf* transcription are mediated by increased histone acetylation within and upstream of the active *Bdnf* exons 1, 4 and 6. As predicted, VPA administered to the pregnant dam at E12.5 induced a robust increase in H3K9/14ac, H3K27ac and H4K5/8/12/16ac at every site examined (Fig. 2). Thus, VPA promoted the histone acetylation indiscriminately at exons Pr1, Ex1, Ex 2, Pr4, Ex4, Pr6 and Ex6. Since enzymatic chromatin fragmentation reduced the average size to 1 – 2 nucleosomes (Supplementary Fig. 1), the separation between the promoter region and 5'UTE amplicons (Supplementary Fig. 3) is sufficient to reflect association with different nucleosomes. Thus, VPA induces a generalized increase in histone acetylation both up- and downstream of multiple TSSs in *Bdnf*.

The increased levels of H3K27ac and H4K5/8/12/16ac at Pr4 and Ex4 returned to baseline within 24 hrs (Fig. 3), tracking the time course of *Bdnf* mRNA and protein [26]. Our results do not support a mechanism by which histone acetylation alone is sufficient for transcription; acetylation may be one of multiple activating marks that are required. However, if histone acetylation is necessary for gene activation, deacetylation observed at 24 hrs may contribute to the termination of *Bdnf* transcription.

Changes in DNA methylation do not mediate the effects of VPA on *Bdnf* in the developing brain

Overall, we found little effect of VPA exposure on DNA CpG methylation of *Bdnf* in the E12.5 fetal brain (Fig. 5C). Indeed, levels of methylation across P1/E1, P4/E4 and P6/E6 were very low (<10%), consistent with a high CpG density (CpG islands) in these regions; in general, low levels of CpG methylation are found early in fetal development and those levels increase later [56]. One possible consequence of the low level of CpG methylation, normally a silencing epigenetic mark, is that during early embryonic development, *Bdnf* needs to be available for rapid activation by transcription factors and histone modifications, which could be impeded if CpG demethylation were also required.

Although 113 of the 117 CpGs in P1/E1, P4/E4 and P6/E6 were not significantly methylated in the control fetal mouse brain, all four CpGs in a cluster upstream from the Ca^{2+}-dependent regulatory elements (CaRE1 – 3) of P4, were substantially methylated (30 – 50%); however, VPA had minimal effect on methylation of those CpGs (Fig. 6). It is of interest that 3 of the 4 CpGs in the cluster are components of a sequence (**`cggaattct`**) that is 80% homologous to a putative regulatory element that binds the transcription factors, Elk1 or ETS. While regulation of *Bdnf* transcription by Elk-1 has previously been reported, direct binding to those DNA sequences has not been observed [57,58]. However, none of those

studies examined neuronal cells; cell type and CpG methylation status may determine whether Elk-1 can bind to *Bdnf*.

A proposed mechanism for sex differences in H3K4me3

Gonadal development and sex hormone expression is just beginning at E12.5 in the mouse [59] with very low levels detected at that time [60]. Consequently, it is likely that the sexually dimorphic regulation of *Bdnf* transcripts is due to genetic sex rather than sex hormones. Our results suggest that the enzymatic machinery involved in H3K4 demethylation may be more active in males than in females; indeed, two H3K4 demethylases are sex-linked. *Kdm5d*, the gene encoding the H3K4-specific demethylase, JARID1D, is located on the Y-chromosome [61] and is expressed only in males, while its homolog, *Kdm5c* (also known as X-linked mental retardation gene), encoding JARID1C is located on the X-chromosome and may, in some tissues and developmental stages, only partially escape X-inactivation [62,63]. A mutation in *Kdm5c* (JARID1C) has been linked to autism [64], underscoring an important role of this enzyme in brain development. Thus, differential expression of JARID1C and D demethylases may contribute to the sex differences we observed in H3K4me3 in *Bdnf* and in *Bdnf* transcripts.

Functional implications of multiple 5'UTEs in *Bdnf*

During transcription, RNA splicing can lead to 18 different transcripts [28], each with the same protein coding region, one of nine distinct 5'UTEs (*c.f.*, Fig. 1A) and either a long or short 3'UTR. There are at least two theories concerning the functional role played by the multiple 5'UTEs. The first proposes that the 5'UTEs function as "zip codes" that specify, during transcription, the spatial domain within the cell to which the mRNA should be targeted, such as the soma or distal dendrites [65,66]. Whether such exon-specific transcript targeting is operating in the proliferating neuroprogenitors or immature neurons that comprise the primary cell types in the fetal brain at E12.5 is not known. The other postulated function of the *Bdnf* 5'UTEs is to enable *Bdnf* transcription activated by multiple, cell-specific signaling pathways [67]. In that case, the cell-specific signaling mechanism would be matched to the regulatory elements in one of the promoter regions of the 5'UTEs. Thus, according to this second theory, expression of transcripts with different 5'UTEs would be specific to cell type, brain region, and/or developmental stage. By either or both of these two mechanisms, sex differences in VPA-induced *Bdnf* levels of Ex1- and Ex4-containing transcripts (Fig. 1B,C), mediated by H3K4me3 (Fig. 4A), could determine the cellular sites of BDNF synthesis. This could alter the trajectory of brain development in males versus females, possibly contributing to sex differences in the occurrence and severity of behavioral symptoms.

Reconciling male sex bias in ASDs with higher VPA-induced *Bdnf* expression in females

In the rodent VPA model, there is a correlation between elevated *Bdnf* expression in the fetal brain [26] and ASD-like symptoms in the adult [15], suggesting a causal link between the two. However, VPA exposure alters expression of a wide range of genes in addition to *Bdnf*, including some that could dysregulate brain development and function if overexpressed in the fetal brain [68]. The results reported here show that, following *in utero* VPA exposure, there is more Ex1- and Ex4- *Bdnf* mRNA in female than in male fetal brains. The lower

incidence and severity of ASDs in females needs to be reconciled with this result. One possibility is that elevated BDNF is not the cause of the symptoms, but instead, acts as a compensating, protective factor in females to offset other pathogenic effects of VPA.

Supplementary Material

Refer to Web version on PubMed Central for supplementary material.

Acknowledgments

The authors gratefully acknowledge support from NIH grant R01HD067135 to BKK and a predoctoral fellowship from the PhRMA Foundation to MAK. We thank Drs. S. G. Dorsey, T. F. Haydar, T. J. Kingsbury, K. Martinowich, M. M. McCarthy, E. M. Powell, A. Puche and R. W. Tsien for comments on the manuscript and C. D. Roby for technical advice. Submitted by M Konopko in partial fulfillment of the requirements for a PhD in Neuroscience from the University of Maryland Baltimore.

Supported by NIH grant R01HD067135 to BKK and a PhRMA predoctoral fellowship to MAK.

References

1. Chawarska K, Macari S, Shic F. Decreased spontaneous attention to social scenes in 6-month-old infants later diagnosed with autism spectrum disorders. Biol Psychiatry. 2013; 74:195–203. [PubMed: 23313640]
2. Surén P, Roth C, Bresnahan M, Haugen M, Hornig M, Hirtz D, et al. Association between maternal use of folic acid supplements and risk of autism spectrum disorders in children. JAMA. 2013; 309:570–577. [PubMed: 23403681]
3. Virk J, Liew Z, Olsen J, Nohr EA, Catov JM, Ritz B. Preconceptional and prenatal supplementary folic acid and multivitamin intake and autism spectrum disorders. Autism Int J Res Pract. 2015; doi: 10.1177/1362361315604076
4. Chang J, Gilman SR, Chiang AH, Sanders SJ, Vitkup D. Genotype to phenotype relationships in autism spectrum disorders. Nat Neurosci. 2015; 18:191–198. [PubMed: 25531569]
5. Budimirovic DB, Kaufmann WE. What can we learn about autism from studying fragile X syndrome? Dev Neurosci. 2011; 33:379–394. [PubMed: 21893949]
6. Arndt TL, Stodgell CJ, Rodier PM. The teratology of autism. Int J Dev Neurosci. 2005; 23:189–199. [PubMed: 15749245]
7. Ploeger A, Raijmakers MEJ, van der Maas HLJ, Galis F. The Association Between Autism and Errors in Early Embryogenesis: What Is the Causal Mechanism? Biol Psychiatry. 2010; 67:602–607. [PubMed: 19932467]
8. Roberts EM, English PB, Grether JK, Windham GC, Somberg L, Wolff C. Maternal residence near agricultural pesticide applications and autism spectrum disorders among children in the California Central Valley. Environ Health Perspect. 2007; 115:1482–1489. [PubMed: 17938740]
9. Wisner KL, Leckman-Westin E, Finnerty M, Essock SM. Valproate prescription prevalence among women of childbearing age. Psychiatr Serv Wash DC. 2011; 62:218–220.
10. Bromley RL, Mawer G, Clayton-Smith J, Baker GA. Autism Spectrum Disorders Following in Utero Exposure to Antiepileptic Drugs. Neurology. 2008; 71:1923–1924. [PubMed: 19047565]
11. Christensen J, Grønborg TK, Sørensen MJ, Schendel D, Parner ET, Pedersen LH, et al. Prenatal valproate exposure and risk of autism spectrum disorders and childhood autism. JAMA. 2013; 309:1696–1703. [PubMed: 23613074]
12. Gerard EE, Meador KJ. An Update on Maternal Use of Antiepileptic Medications in Pregnancy and Neurodevelopment Outcomes. J Pediatr Genet. 2015; 4:94–110. [PubMed: 27617120]
13. Moore SJ, Turnpenny P, Quinn A, Glover S, Lloyd DJ, Montgomery T, et al. A clinical study of 57 children with fetal anticonvulsant syndromes. J Med Genet. 2000; 37:489–497. [PubMed: 10882750]

14. Ornoy A, Weinstein-Fudim L, Ergaz Z. Prenatal factors associated with autism spectrum disorder (ASD). Reprod Toxicol Elmsford N. 2015; 56:155–169.
15. Roullet FI, Lai JKY, Foster JA. In utero exposure to valproic acid and autism — A current review of clinical and animal studies. Neurotoxicol Teratol. 2013; 36:47–56. [PubMed: 23395807]
16. Mychasiuk R, Richards S, Nakahashi A, Kolb B, Gibb R. Effects of rat prenatal exposure to valproic acid on behaviour and neuro-anatomy. Dev Neurosci. 2012; 34:268–276. [PubMed: 22890088]
17. Gandal MJ, Edgar JC, Ehrlichman RS, Mehta M, Roberts TPL, Siegel SJ. Validating γ oscillations and delayed auditory responses as translational biomarkers of autism. Biol Psychiatry. 2010; 68:1100–1106. [PubMed: 21130222]
18. Schneider T, Przewłocki R. Behavioral alterations in rats prenatally exposed to valproic acid: animal model of autism. Neuropsychopharmacol. 2005; 30:80–89.
19. Hutsler JJ, Zhang H. Increased dendritic spine densities on cortical projection neurons in autism spectrum disorders. Brain Res. 2010; 1309:83–94. [PubMed: 19896929]
20. Kataoka S, Takuma K, Hara Y, Maeda Y, Ago Y, Matsuda T. Autism-like behaviours with transient histone hyperacetylation in mice treated prenatally with valproic acid. Int J Neuropsychopharmacol. 2013; 16:91–103. [PubMed: 22093185]
21. Stoner R, Chow ML, Boyle MP, Sunkin SM, Mouton PR, Roy S, et al. Patches of disorganization in the neocortex of children with autism. N Engl J Med. 2014; 370:1209–1219. [PubMed: 24670167]
22. Codagnone MG, Podestá MF, Uccelli NA, Reinés A. Differential Local Connectivity and Neuroinflammation Profiles in the Medial Prefrontal Cortex and Hippocampus in the Valproic Acid Rat Model of Autism. Dev Neurosci. 2015; 37:215–231. [PubMed: 25895486]
23. Schneider T, Roman A, Basta-Kaim A, Kubera M, Budziszewska B, Schneider K, et al. Gender-specific behavioral and immunological alterations in an animal model of autism induced by prenatal exposure to valproic acid. Psychoneuroendocrinology. 2008; 33:728–740. [PubMed: 18396377]
24. Mowery TM, Wilson SM, Kostylev PV, Dina B, Buchholz JB, Prieto AL, et al. Embryological exposure to valproic acid disrupts morphology of the deep cerebellar nuclei in a sexually dimorphic way. Int J Dev Neurosci. 2015; 40:15–23. [PubMed: 25447790]
25. Kim KC, Kim P, Go HS, Choi CS, Park JH, Kim HJ, et al. Male-specific alteration in excitatory post-synaptic development and social interaction in pre-natal valproic acid exposure model of autism spectrum disorder. J Neurochem. 2013; 124:832–843. [PubMed: 23311691]
26. Almeida LEF, Roby CD, Krueger BK. Increased BDNF expression in fetal brain in the valproic acid model of autism. Mol Cell Neurosci. 2014; 59:57–62. [PubMed: 24480134]
27. Cohen-Cory S, Kidane AH, Shirkey NJ, Marshak S. Brain-derived neurotrophic factor and the development of structural neuronal connectivity. Dev Neurobiol. 2010; 70:271–288. [PubMed: 20186709]
28. Aid T, Kazantseva A, Piirsoo M, Palm K, Timmusk T. Mouse and rat BDNF gene structure and expression revisited. J Neurosci Res. 2007; 85:525–535. [PubMed: 17149751]
29. Delcuve GP, Khan DH, Davie JR. Roles of histone deacetylases in epigenetic regulation: emerging paradigms from studies with inhibitors. Clin Epigenetics. 2012; 4:5. [PubMed: 22414492]
30. Monti B, Polazzi E, Contestabile A. Biochemical, molecular and epigenetic mechanisms of valproic acid neuroprotection. Curr Mol Pharmacol. 2009; 2:95–109. [PubMed: 20021450]
31. Hezroni H, Sailaja BS, Meshorer E. Pluripotency-related, valproic acid (VPA)-induced genome-wide histone H3 lysine 9 (H3K9) acetylation patterns in embryonic stem cells. J Biol Chem. 2011; 286:35977–35988. [PubMed: 21849501]
32. Karmodiya K, Krebs AR, Oulad-Abdelghani M, Kimura H, Tora L. H3K9 and H3K14 acetylation co-occur at many gene regulatory elements, while H3K14ac marks a subset of inactive inducible promoters in mouse embryonic stem cells. BMC Genomics. 2012; 13:424. [PubMed: 22920947]
33. Yao B, Christian KM, He C, Jin P, Ming G-L, Song H. Epigenetic mechanisms in neurogenesis. Nat Rev Neurosci. 2016; 17:537–549. [PubMed: 27334043]

34. Kumamaru E, Egashira Y, Takenaka R, Takamori S. Valproic acid selectively suppresses the formation of inhibitory synapses in cultured cortical neurons. Neurosci Lett. 2014; 569:142–147. [PubMed: 24708928]
35. Moldrich RX, Leanage G, She D, Dolan-Evans E, Nelson M, Reza N, Reutens DC. Inhibition of histone deacetylase in utero causes sociability deficits in postnatal mice. Behav Brain Res. 2013; 257:253–264. [PubMed: 24103642]
36. Ishimaru N, Fukuchi M, Hirai A, Chiba Y, Tamura T, Takahashi N, et al. Differential epigenetic regulation of BDNF and NT-3 genes by trichostatin A and 5-aza-2'-deoxycytidine in Neuro-2a cells. Biochem Biophys Res Commun. 2010; 394:173–177. [PubMed: 20188708]
37. Suganuma T, Workman JL. Crosstalk among Histone Modifications. Cell. 2008; 135:604–607. [PubMed: 19013272]
38. Berger SL. The complex language of chromatin regulation during transcription. Nature. 2007; 447:407–412. [PubMed: 17522673]
39. Schaafsma SM, Pfaff DW. Etiologies underlying sex differences in Autism Spectrum Disorders. Front Neuroendocrinol. 2014; 35:255–271. [PubMed: 24705124]
40. Lubin FD, Roth TL, Sweatt JD. Epigenetic regulation of BDNF gene transcription in the consolidation of fear memory. J Neurosci. 2008; 28:10576–10586. [PubMed: 18923034]
41. Martinowich K, Hattori D, Wu H, Fouse S, He F, Hu Y, et al. DNA methylation-related chromatin remodeling in activity-dependent BDNF gene regulation. Science. 2003; 302:890–893. [PubMed: 14593184]
42. Ratnu VS, Emami MR, Bredy TW. Genetic and epigenetic factors underlying sex differences in the regulation of gene expression in the brain. J Neurosci Res. 2017; 95:301–310. [PubMed: 27870402]
43. Richardson L, Venkataraman S, Stevenson P, Yang Y, Moss J, Graham L, et al. EMAGE mouse embryo spatial gene expression database: 2014 update. Nucleic Acids Res. 2014; 42:D835–D844. [PubMed: 24265223]
44. Umlauf, D., Goto, Y., Wagschal, A., Arnaud, P., Feil, R., Lewis, A. [cited 2016 Oct 7] Epigenome NoE - protocol: Chromatin immunoprecipitation on native chromatin from cells and tissues. Epigenome Netw Excell. 2005. Available from: http://www.epigenome-noe.net/researchtools/protocol.php_protid=22.html
45. Chen WG, West AE, Tao X, Corfas G, Szentirmay MN, Sawadogo M, et al. Upstream stimulatory factors are mediators of Ca2+-responsive transcription in neurons. J Neurosci Off J Soc Neurosci. 2003; 23:2572–2581.
46. Du J, Patel DJ. Structural biology-based insights into combinatorial readout and crosstalk among epigenetic marks. Biochim Biophys Acta BBA - Gene Regul Mech. 2014; 1839:719–727.
47. Huang P-H, Plass C, Chen C-S. Effects of Histone Deacetylase Inhibitors on Modulating H3K4 Methylation Marks – A Novel Cross-Talk Mechanism between Histone-Modifying Enzymes. Mol Cell Pharmacol. 2011; 3:39–43. [PubMed: 22468166]
48. Nightingale KP, Gendreizig S, White DA, Bradbury C, Hollfelder F, Turner BM. Cross-talk between Histone Modifications in Response to Histone Deacetylase Inhibitors MLL4 LINKS HISTONE H3 ACETYLATION AND HISTONE H3K4 METHYLATION. J Biol Chem. 2007; 282:4408–4416. [PubMed: 17166833]
49. Harikumar A, Meshorer E. Chromatin remodeling and bivalent histone modifications in embryonic stem cells. EMBO Rep. 2015; doi: 10.15252/embr.201541011
50. Cedar H, Bergman Y. Linking DNA methylation and histone modification: patterns and paradigms. Nat Rev Genet. 2009; 10:295–304. [PubMed: 19308066]
51. Kondo Y. Epigenetic cross-talk between DNA methylation and histone modifications in human cancers. Yonsei Med J. 2009; 50:455–463. [PubMed: 19718392]
52. Vaissière T, Sawan C, Herceg Z. Epigenetic interplay between histone modifications and DNA methylation in gene silencing. Mutat Res Mutat Res. 2008; 659:40–48. [PubMed: 18407786]
53. Sugathan A, Waxman DJ. Genome-wide analysis of chromatin states reveals distinct mechanisms of sex-dependent gene regulation in male and female mouse liver. Mol Cell Biol. 2013; 33:3594–3610. [PubMed: 23836885]

54. Shen EY, Ahern TH, Cheung I, Straubhaar J, Dincer A, Houston I, et al. Epigenetics and sex differences in the brain: A genome-wide comparison of histone-3 lysine-4 trimethylation (H3K4me3) in male and female mice. Exp Neurol. 2015; 268:21–29. [PubMed: 25131640]
55. Sachs M, Onodera C, Blaschke K, Ebata KT, Song JS, Ramalho-Santos M. Bivalent chromatin marks developmental regulatory genes in the mouse embryonic germline in vivo. Cell Rep. 2013; 3:1777–1784. [PubMed: 23727241]
56. Lister R, Mukamel EA, Nery JR, Urich M, Puddifoot CA, Johnson ND, et al. Global epigenomic reconfiguration during mammalian brain development. Science. 2013; 341:1237905. [PubMed: 23828890]
57. Boros J, Donaldson IJ, O'Donnell A, Odrowaz ZA, Zeef L, Lupien M, et al. Elucidation of the ELK1 target gene network reveals a role in the coordinate regulation of core components of the gene regulation machinery. Genome Res. 2009; 19:1963–1973. [PubMed: 19687146]
58. Odrowaz Z, Sharrocks AD. ELK1 Uses Different DNA Binding Modes to Regulate Functionally Distinct Classes of Target Genes. PLoS Genet. 2012; 8:e1002694. [PubMed: 22589737]
59. Steinberger, A., Steinberger, E. Testicular Development, Structure, and Function. Raven Press; 1980.
60. Habert R, Picon R. Testosterone, dihydrotestosterone and estradiol-17 beta levels in maternal and fetal plasma and in fetal testes in the rat. J Steroid Biochem. 1984; 21:193–198. [PubMed: 6482429]
61. Wolstenholme JT, Rissman EF, Bekiranov S. Sexual differentiation in the developing mouse brain: contributions of sex chromosome genes. Genes Brain Behav. 2013; 12:166–180. [PubMed: 23210685]
62. Sheardown S, Norris D, Fisher A, Brockdorff N. The Mouse Smcx Gene Exhibits Developmental and Tissue Specific Variation in Degree of Escape from X Inactivation. Hum Mol Genet. 1996; 5:1355–1360. [PubMed: 8872477]
63. Yang F, Babak T, Shendure J, Disteche CM. Global survey of escape from X inactivation by RNA-sequencing in mouse. Genome Res. 2010; 20:614–622. [PubMed: 20363980]
64. Adegbola A, Gao H, Sommer S, Browning M. A novel mutation in JARID1C/SMCX in a patient with autism spectrum disorder (ASD). Am J Med Genet A. 2008; 146A:505–511. [PubMed: 18203167]
65. Baj G, Leone E, Chao MV, Tongiorgi E. Spatial segregation of BDNF transcripts enables BDNF to differentially shape distinct dendritic compartments. Proc Natl Acad Sci U S A. 2011; 108:16813–16818. [PubMed: 21933955]
66. Maynard KR, Hill JL, Calcaterra NE, Palko ME, Kardian A, Paredes D, et al. Functional role of BDNF production from unique promoters in aggression and serotonin signaling. Neuropsychopharmacol. 2016; 41:1943–1955.
67. Maynard KR, Hobbs JW, Sukumar M, Kardian AS, Jimenez DV, Schloesser RJ, Martinowich K. Bdnf mRNA splice variants differentially impact CA1 and CA3 dendrite complexity and spine morphology in the hippocampus. Brain Struct Funct. 2017 [Epub ahead of print].
68. Kawanai T, Ago Y, Watanabe R, Inoue A, Taruta A, Onaka Y, et al. Prenatal Exposure to Histone Deacetylase Inhibitors Affects Gene Expression of Autism-Related Molecules and Delays Neuronal Maturation. Neurochem Res. 2016; 41:2574–2584. [PubMed: 27300699]

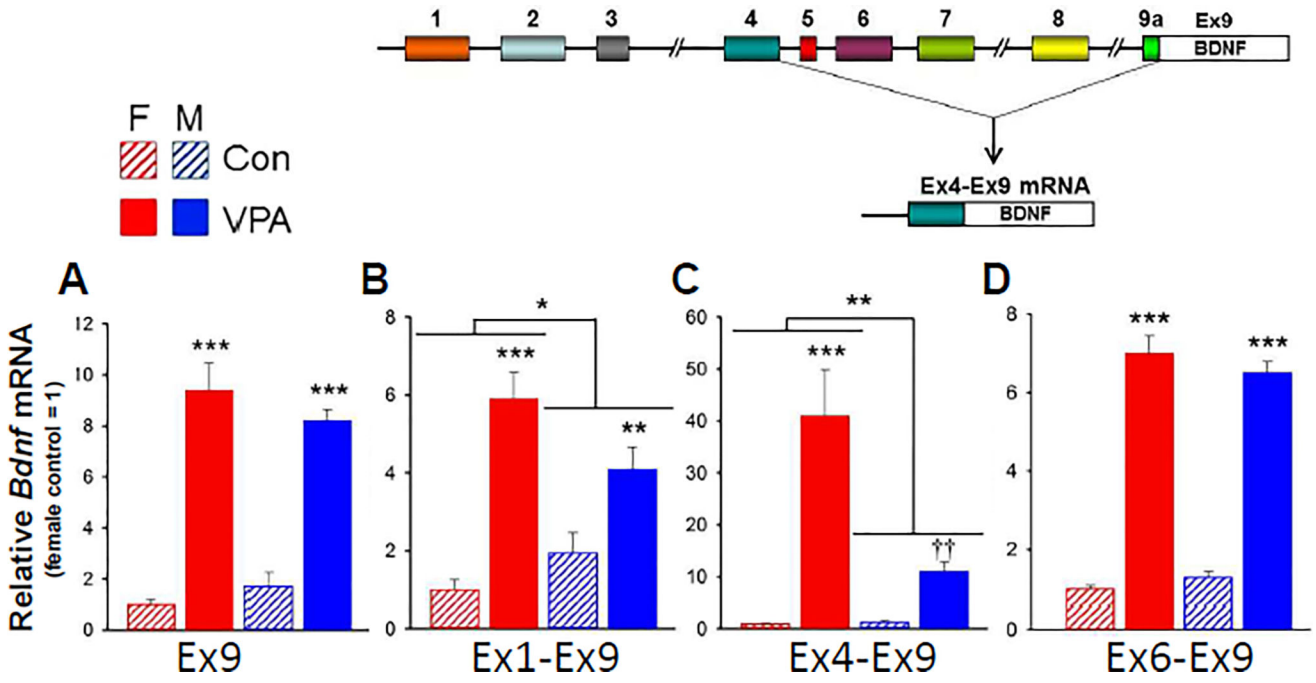

Fig. 1. Effect of VPA exposure on *Bdnf* mRNA levels in fetal brain

RNA was measured by qRT-PCR (see Supplementary Table 1B for primer sequences). Data were corrected for β-actin expression in each sample. Expression levels were normalized to the female control for each target. **A**. Effect of VPA on expression of Ex9 mRNA in male and female fetal brains. n = 6. **B–D**. Effect of VPA on expression of Ex1-, Ex4- and Ex6-containing *Bdnf* transcripts in male and female fetal brains. Two-way ANOVA: *, $p<0.05$; **, $p<0.01$; ***, $p<0.001$. Effect of VPA on *Bdnf4* in males failed Tukey test; ††: significantly different form control, $p<0.01$ by t-test. n = 6. Full statistical analysis is reported in Supplementary Table 2. **Inset** (Modified from Aid et al., 2007): Mouse *Bdnf* consists of nine 5'UTEs upstream from the single protein coding exon (Ex9). Thin lines represent introns. During *Bdnf* transcription, one of the 5'UTEs is spliced to Ex9 as illustrated for Ex4 mRNA.

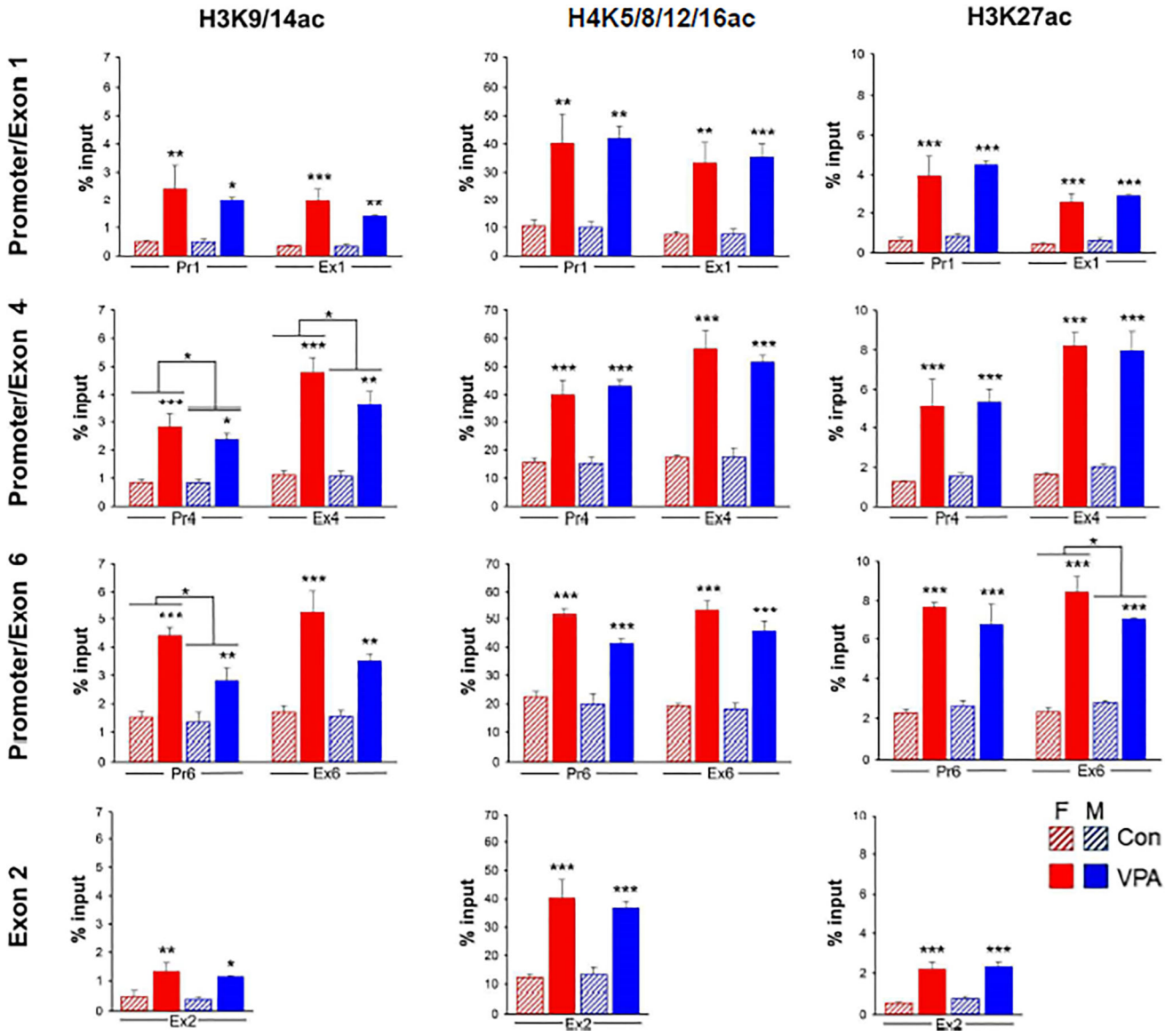

Fig. 2. VPA-induced histone acetylation in *Bdnf*

Data were generated by native ChIP and are expressed as the percent of total chromatin associated with the indicated histone modification (% input) in each column. Pr1, Pr4 and Pr6 are promoter regions upstream from the TSS of exons 1, 4, and 6 respectively. Ex1, Ex2, Ex4 and Ex6 are located in the 5'UTEs downstream from the TSSs. The locations of the amplicons analyzed are shown in Supplementary Fig. 3. VPA-induced acetylation at H3K9/14 was slightly greater in females at H3K9/14 in Pr4, Ex4 and Pr6 and at H3K27ac in Ex6. Data were analyzed by 2-way ANOVA with sex and treatment as variables. Two-way ANOVA; *, $p<0.05$; **, $p<0.01$; ***, $p<0.001$. n = 3 pooled samples (c.f., Materials and Methods). Full statistical analysis is shown in Supplementary Table 3.

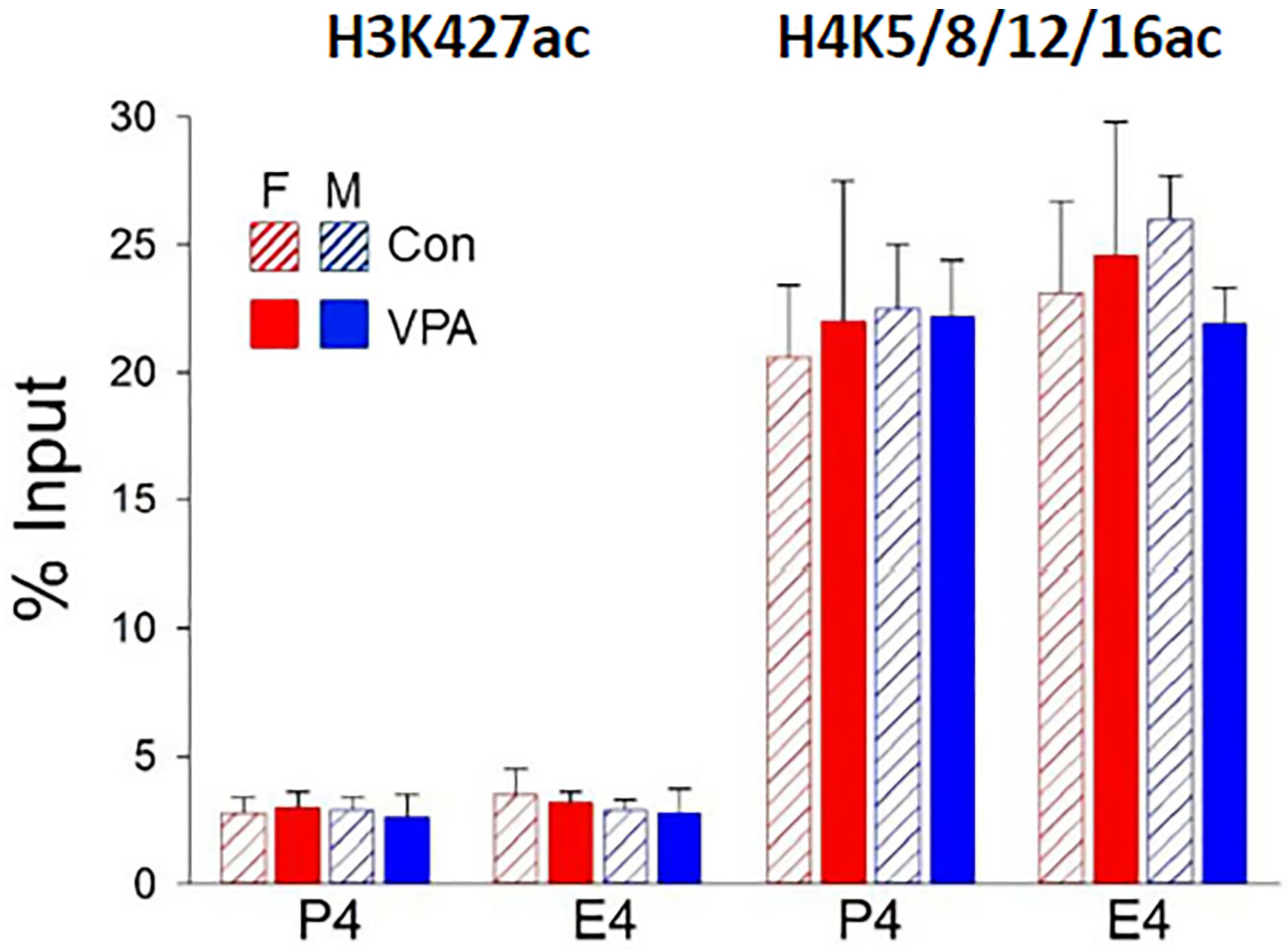

Fig. 3. Stimulation of H3K27ac and H4Kac by VPA reversed by 24 hr

Acetylation at all sites studied had reversed by 24hrs. No significant effect of treatment (VPA) or sex by two-way ANOVA. n = 3 pooled samples.

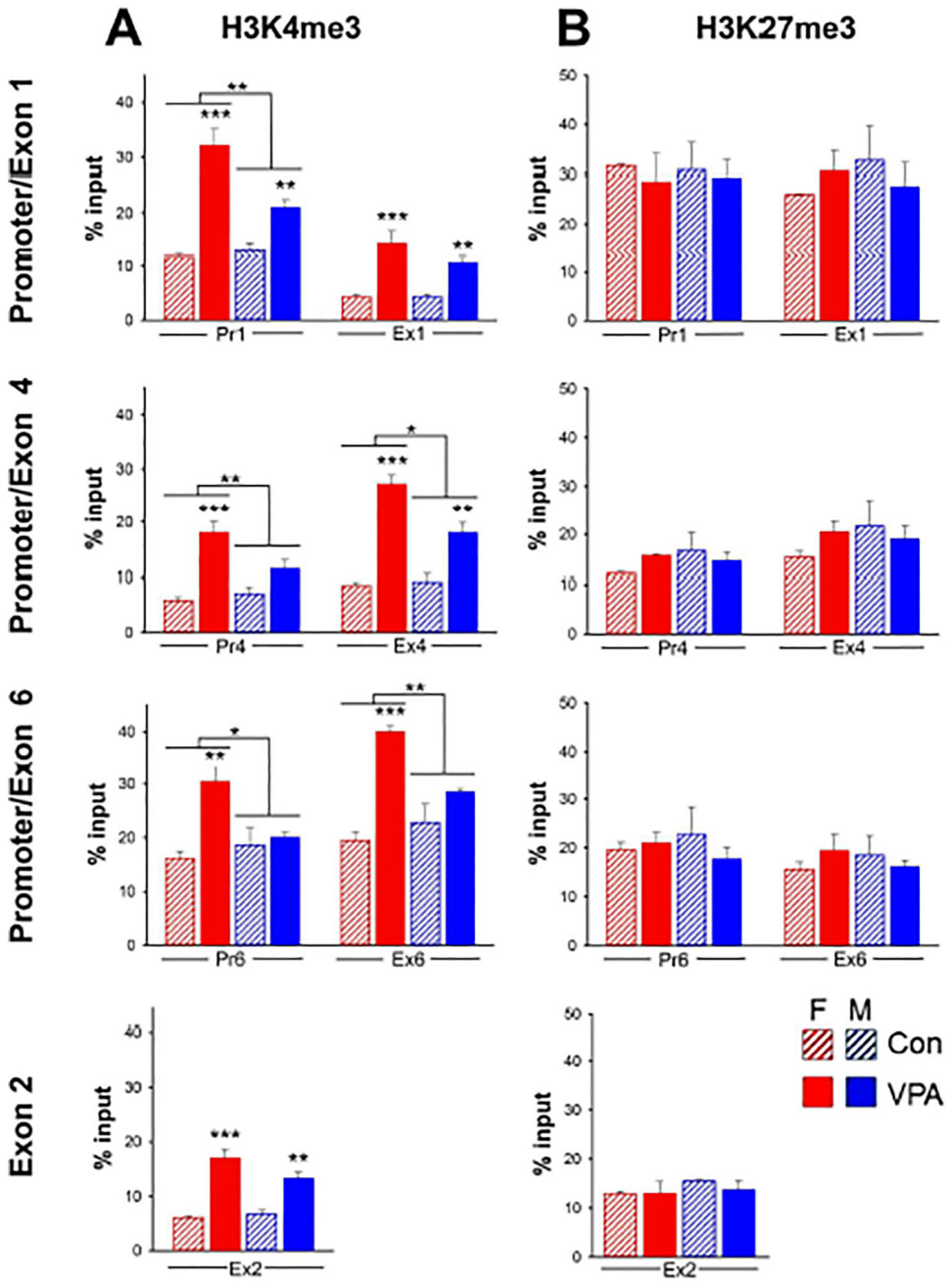

Fig. 4. Sex differences in VPA induced levels of *Bdnf* H3K4me3

A: Effect of VPA on H3K4me3. The level of H3K4me3 following VPA exposure was significantly lower in males than in females at all regions examined except Ex1 and Ex2. VPA did not affect H3K4me3 in males at Pr4, Pr6 and Ex6. n = 6 pooled samples. Two-way ANOVA; *, $p<0.05$; **, $p<0.01$; ***, $p<0.001$. Full statistical analysis is shown in Supplementary Table 4. **B**: Effect of VPA on H3K27me3. There was no significant effect of VPA in either males or females. n = 3 pooled samples.

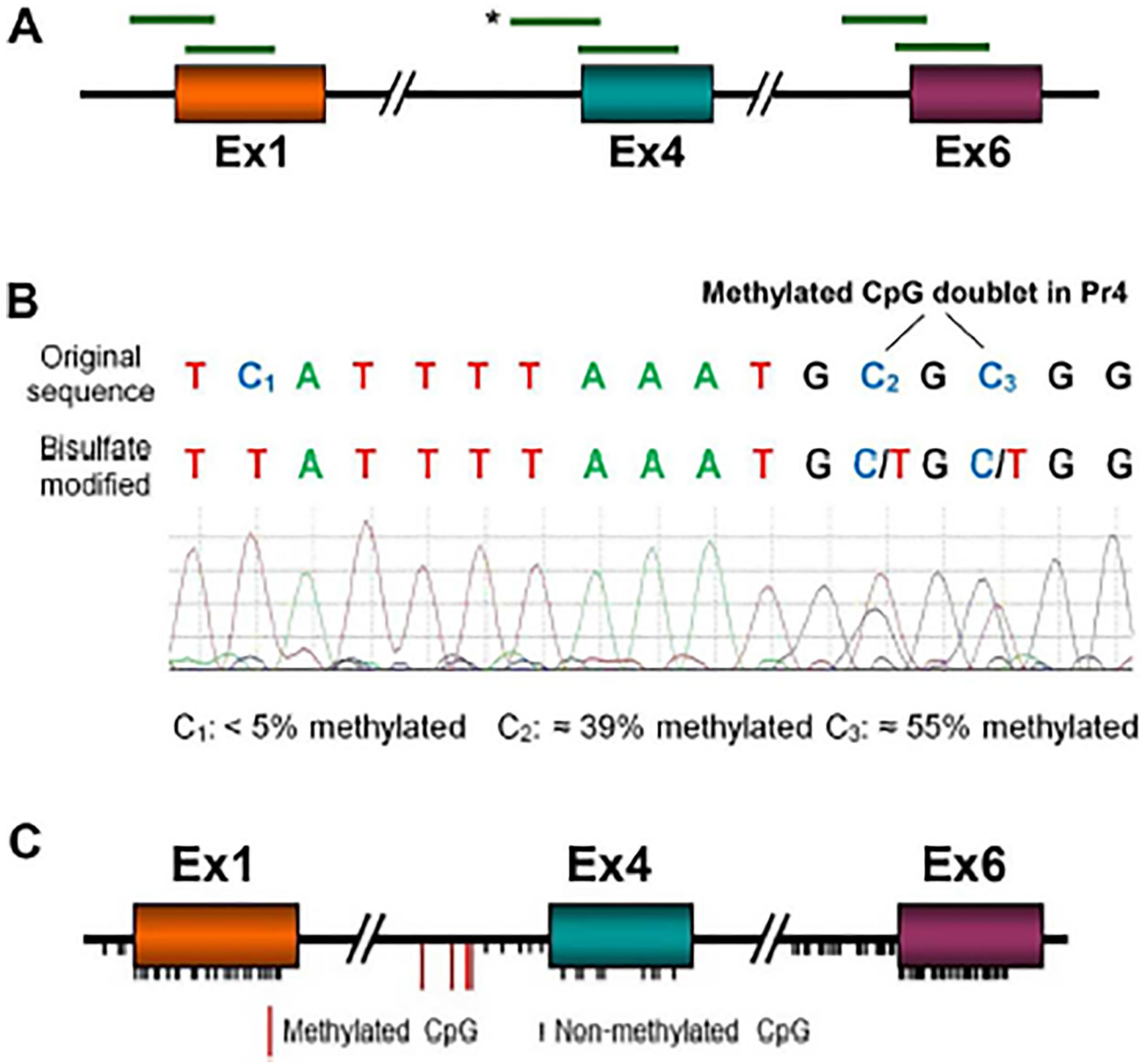

Fig. 5. DNA CpG methylation in the vicinity of *Bdnf* exon 1, 4 and 6 TSSs

A. Overlapping sequences of bisulfite-modified DNA from control and VPA-treated fetal brains. See Supplementary Table 1D for primer sequences. **B**. Typical results showing the Sanger sequencing chromatogram of the sequence in *Bdnf* P4 indicated by * in A. The original and bisulfite-converted sequences are shown. Cytosines −111 (C_2) and −109 (C_3) were read as 39% and 55% cytosine (methylated). With the exception of cytosines −205, −148, −111- and − 109, all Cs, both CpGs and non-CpGs, read as >90% T indicating that they were not significantly methylated (e.g., C_1). VPA: n = 6, Control: n = 8. **C**. Summary of the locations of the CpGs examined, which comprise all the CpGs in the indicated sequences. Black ticks represent unmethylated CpGs; red ticks represent CpGs −205, −148, −111 and −109 in P4, which were 30 – 60% methylated (see Fig. 6B).

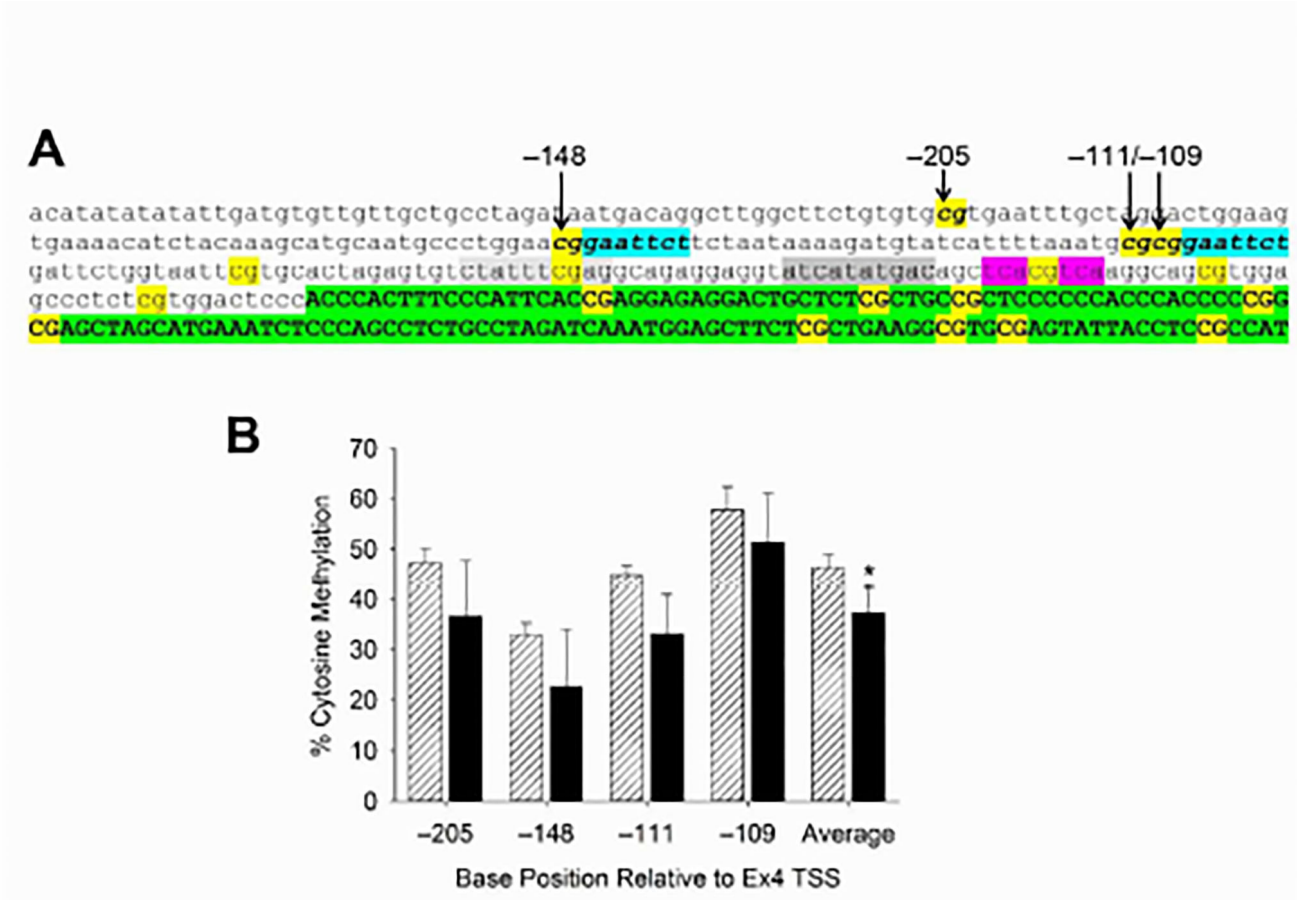

Fig. 6. Hyper-methylated CpG cluster in *Bdnf* P4

A. CpGs are indicated in yellow. The four CpGs in the hyper-methylated cluster are indicated in **bold**. The Ca^{2+}-dependent regulatory elements, designated CaRE1–3 in *Bdnf* Pr4, are highlighted in light gray, dark gray and pink, respectively. Blue highlighting indicates the downstream sequence of two putative Elk-1 binding sites (***cggaattct***). The 5'UTE (Ex4) is indicated in green highlighting. **B**. Effects of VPA exposure on E12.5 on the level of cytosine methylation is shown for each CpG in the cluster. Control methylation ranged from 32% to 58%. There was no significant effect of VPA on any single CpG; the aggregate level of CpG methylation across the cluster was reduced by 20%. *, p<.05 (t-test). VPA: n = 6, Control: n = 8.